High-Resolution Maps of Bathymetry and Benthic Habitats in Shallow-Water Environments Using Multispectral Remote Sensing Imagery

Francisco Eugenio, *Senior Member, IEEE*, Javier Marcello, *Senior Member, IEEE*, and Javier Martin

Abstract—Coastlines, shoals, and reefs are some of the most dynamic and constantly changing regions of the globe. The emergence of high-resolution satellites with new spectral channels, such as the WorldView-2, increases the amount of data available, thereby improving the determination of coastal management parameters. Water-leaving radiance is very difficult to determine accurately, since it is often small compared to the reflected radiance from other sources such as atmospheric and water surface scattering. Hence, the atmospheric correction has proven to be a very important step in the processing of high-resolution images for coastal applications. On the other hand, specular reflection of solar radiation on nonflat water surfaces is a serious confounding factor for bathymetry and for obtaining the seafloor albedo with high precision in shallow-water environments. This paper describes, at first, an optimal atmospheric correction model, as well as an improved algorithm for sunglint removal based on combined physical and image processing techniques. Then, using the corrected multispectral data, an efficient multichannel physics-based algorithm has been implemented, which is capable of solving through optimization the radiative transfer model of seawater for bathymetry retrieval, unmixing the water intrinsic optical properties, depth, and seafloor albedo contributions. Finally, for the mapping of benthic features, a supervised classification methodology has been implemented, combining seafloor-type normalized indexes and support vector machine techniques. Results of atmospheric correction, remote bathymetry, and benthic habitat mapping of shallow-water environments have been validated with *in situ* data and available bionomic profiles providing excellent accuracy.

Index Terms—Atmospheric model, bathymetry mapping, benthic habitat mapping, high-resolution multispectral imagery, physical and image processing techniques, sunglint, WorldView-2 (WV2).

F. Eugenio and J. Marcello are with the Instituto de Oceanografía y Cambio Global, Universidad de Las Palmas de Gran Canaria, Campus Universitario de Tafira, 35017 Las Palmas de Gran Canaria, Spain (e-mail: feugenio@dsc.ulpgc.es).

J. Martin was with the Instituto de Oceanografía y Cambio Global, Universidad de Las Palmas de Gran Canaria, Campus Universitario de Tafira, 35017 Las Palmas de Gran Canaria, Spain. He is now with the Spanish Aerospace Defense Administration (Instituto Nacional de Tecnica Aeroespacial), 28850 Madrid, Spain.

Color versions of one or more of the figures in this paper are available online at http://ieeexplore.ieee.org.

I. INTRODUCTION

CURRENTLY, remote spectral imaging of coastal areas can provide valuable information for characterizing and monitoring optically shallow waters. Recent satellite technologies and image processing algorithms have presented the opportunity to develop quantitative techniques that have the potential to improve upon traditional photointerpretation techniques, in terms of cost, mapping fidelity, and objectivity [1]. In many image processing applications using satellite images and specifically in those related to remote sensing of coastal environments, it is necessary to compare multiple images of the same scene acquired by different sensors, or images taken by the same sensor but at different time instants. Typical applications include multitemporal classification, recognition and tracking of specific patterns, multisensor data fusion, analysis of marine ecosystem processes, and environment monitoring. Hence, with the advent of very high-resolution multispectral imaging sensors, there is the potential to retrieve much more information. Applications include water quality monitoring, remote bathymetry, and benthic habitat mapping in littoral zones [2]–[4].

The multispectral information provided by the high-resolution WorldView-2 (WV2) satellite and the ability to change its viewing angle has highlighted the importance of accurately modeling the radiometric and atmospheric effects for shallow-water applications due to the low signal-to-noise ratio available at sensor level on shorter wavelengths. In fact, reflectance of the objects recorded by satellite sensors is generally low and affected by atmospheric absorption and scattering, sensor-target-illumination geometry, and sensor calibration [5]. In the present work, the critical preprocessing steps have been improved to properly use the multispectral data. Hence, atmospheric correction in the littoral zone was advanced through new capabilities added to the Second Simulation of a Satellite Signal in the Solar Spectrum (6S) atmospheric correction method. During this study, we compared the adapted 6S model with coincident ground-based reflectance measurements, in the selected area, analyzing detailed the correlation between the reflectivity values obtained by *in situ* measurements (spectro-radiometer Vis/NIR), and the corresponding values acquired by atmospheric processing of the eight multispectral satellite channels.

The remote bathymetry and mapping of benthic features can be seriously impeded by the specular reflection of solar radiation on nonflat water surfaces [6]. To overcome this challenge, experts could refer to previous methods and models

designed to take advantage of the glint to compute surface characteristics (e.g., wave height) or to remove glint contamination prior to estimating water column constituents and optical properties [7]. As part of the WV2 preprocessing chain, a deglinting algorithm was implemented to properly remove sea surface effects from high-resolution imagery in shallow-water environments prior to estimating seafloor reflectivity. This procedure exploits physical information, but it is also relies on image processing algorithms to achieve the maximum performance.

The problem of estimating water depths using a radiative model has yielded good results because it considers the physical phenomena of water absorption and backscattering and the relationship between the albedo of the seafloor and the reflectivity of the shallow waters [6], [8]. In addition, optical remote bathymetry requires representations of the water-leaving reflectance spectrum as a function of depth for realistic bottom materials and water composition [8], [9]. In this paper, we have developed a multichannel physics-based algorithm to obtain high-resolution remote sensing bathymetry of shallow coastal waters. Hence, the novelty of the spectral capabilities of WV2 multispectral imagery is fully exploited for bathymetry retrieval. Incorporation of accurate bathymetric information is fundamental in benthic habitat modeling.

Benthic habitat mapping provides a means for assessing, for example, the seagrass health by monitoring the spatial distribution and density of seagrass in coastal waters. The capacity to accurately and reliably map and monitor these benthic environments is fundamental for developing management applications, i.e., the Port of Granadilla (Tenerife, Canary Islands) Environmental Monitoring Program. Remote sensing is useful for monitoring shallow coastal ecosystems with clear water, due to good light penetration and easily accessible field data. For derivation of bottom depth or bottom features, in turbid coastal environments, the effects of the water column have to be accounted for. Due to multiple scattering, the remotely measured signal is an integration of that from the water column and that from the bottom. Sophisticated models and methods are required to adequately separate individual signals [4], [10], [11]. Satellite imagery-based spatially enhanced image processing techniques were found to provide a consistent, quantitative, and cost-effective alternative for benthic mapping using enhanced satellite classification when compared to aerial photointerpretation [11].

Integrated spatial and spectral processing techniques were identified as an alternative method for mapping benthos types, extent, and density from WV2 satellite images of the Canary Islands coastal area [12]. A combination of water column correction, seafloor-type normalized indexes, and supervised classification techniques provided the benthic habitat map with high spatial detail and accuracy. In our context, the supervised classification method selected was the support vector machine (SVM) [13]. The SVM was applied to WV2 corrected channels and benthic indexes previously estimated. The training classes were clearly defined, and a separability assessment was conducted using the Jeffries–Matusita distance. Finally, performance evaluation was accomplished using the confusion matrix and the kappa coefficient.
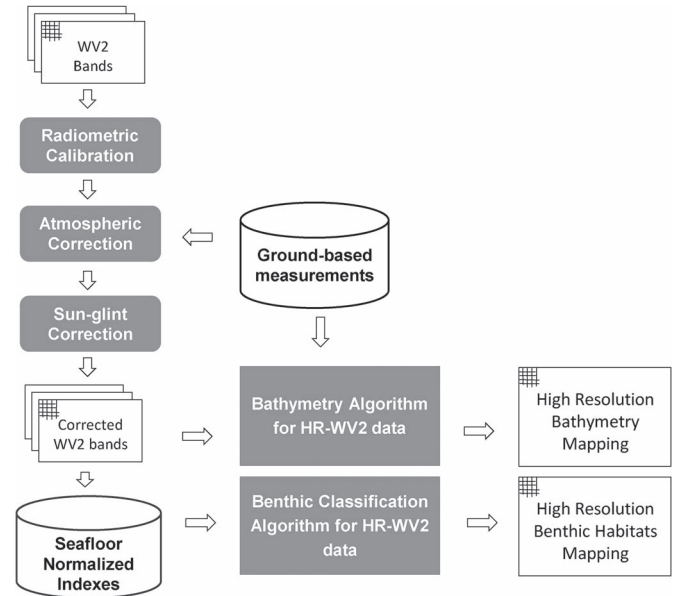

Fig. 1. Schematic procedure of the proposed multispectral WV2 processing chain for high-resolution bathymetry retrieval and benthic mapping.

In summary, a complete high spatial resolution WV2 data processing strategy has been developed for monitoring shallow-water environments, as shown in Fig. 1, and their critical elements have been explored. The processing chain presented in this paper consists in the following:

1) *preprocessing:* an optimal atmospheric correction model and an improved algorithm for sunglint removal based on physical and image processing techniques;
2) *high-resolution bathymetry and benthic habitat mapping:* the integration of the high-resolution WV2 derivate bathymetry, based on a novel multichannel physics-based algorithm capable of solving through optimization the radiative transfer model of seawater; the generation of seafloor-type normalized indexes and the image classification approach to obtain a high-resolution benthic habitat mapping.

This paper is organized as follows: Section II discusses the multispectral high-resolution data preprocessing, specifically the atmospheric and deglinting correction models. Section III focuses on the bathymetry mapping of shallow-water environments, describing the multichannel physics-based algorithm. In Section IV, the procedure for benthic mapping of coastal areas is presented and analyzed. The final conclusions are included in Section V.

II. WV2 MULTISPECTRAL DATA PROCESSING

1) Satellite Image Data Acquisition: The WV2 high-resolution commercial imaging satellite was launched on October 8, 2009, from Vandenberg Air Force Base, and was declared to be operating at full capability on January 4, 2010. The satellite is in a nearly circular sun-synchronous orbit with a period of 100.2 min, an altitude of approximately 770 km, and with a descending nodal crossing time of approximately 10:30 A.M. The WV2 acquires 11-bit data in nine spectral
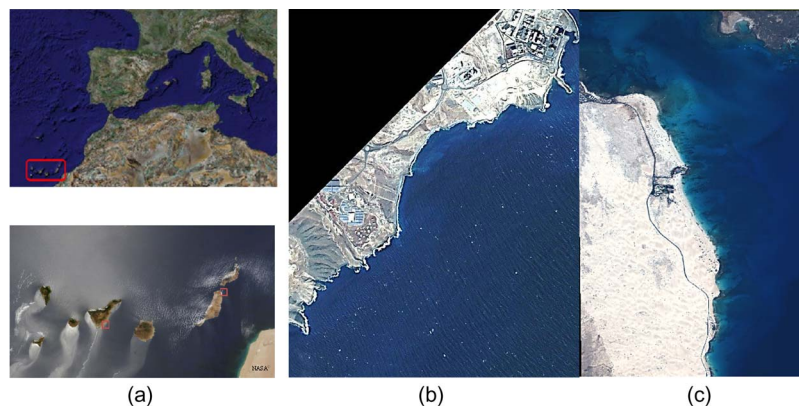
Fig. 2. (a) Location of study areas (Canary Islands)[1] and (b), (c) WorldView-2 images of two Canary Islands coastal areas. (b) Granadilla (Tenerife Island) area. (c) Corralejo (Fuerteventura Island)[2] area.

bands covering panchromatic, coastal, blue, green, yellow, red, red edge, NIR1, and NIR2 [14].

This work relied on Ortho Ready Standard WV2 images. At nadir, the collected nominal ground sample distance is 0.46 m (panchromatic) and 1.84 m (multispectral). Commercially available products are resampled to 0.5 m (panchromatic) and 2.0 m (multispectral). The nominal swath width is 16.4 km. Hence, WV2 satellite provides finer spatial resolution and more spectral information in the visible spectrum than previous satellites, positioning it as the forerunner for oceanographic parameters mapping. However, achieving these goals requires overcoming a number of challenges.

The study area is the Canary Islands[1] coastal environment, which is off the northwest African coast, as shown in Fig. 2. In addition, in Fig. 2, two high-resolution images acquired by WV2 satellite of two different Canary Islands coastal areas, namely, Granadilla (Tenerife Island) and Corralejo (Fuerteventura Island),[2] are presented. Hence, the Port of Granadilla Environmental Monitoring Program was established in 2010, in order to ensure sustained environmental quality across the wide range of natural and artificially created habitats within and immediately outside of the port during it construction. On the other hand, the Corralejo area and Lobo island (Fuerteventura Island) is a biosphere reserve by United Nations Educational, Scientific and Cultural Organizations (UNESCO) and natural protected area, respectively.

2) Atmospheric and Deglinting Correction Models: Water-leaving radiance is very difficult to determine accurately, since it is often small compared to the reflected radiance from other sources such as atmospheric and water surface scattering, and it is subject to uncertainties in the sensor's radiometric calibration. Thus, the atmospheric correction has proven to be a crucial aspect in the processing of high-resolution images that can affect subsequent steps in remote sensing applications of satellite data [5], [15]. On the other hand, specular reflection of solar radiation on nonflat water surfaces is a serious confounding factor for the mapping of biological and physical parameters

in shallow-water environments [7], [16]. Next, we briefly describe the implemented atmospheric correction model and the physical-based algorithm and image processing techniques for sunglint removal, and we present, as well, sample results.

A. Atmospheric Correction Algorithm

Atmospheric correction algorithms to process remotely sensed data from low-resolution sensors [e.g., MODIS, Sea-Viewing Wide Field-of-view Sensor (SeaWiFS), and MEdium Resolution Imaging Spectrometer (MERIS)] were primarily designed for retrieving water-leaving radiances in the visible spectral region over deep ocean areas (Case 1 waters), where the water-leaving radiances are close to zero. For turbid coastal environments and optically shallow waters, water-leaving radiances may be significantly greater than zero because of backscattering by suspended materials in the water and bottom reflectance. Hence, applications of the Case 1 algorithm to satellite imagery acquired over turbid coastal waters often result in negative water-leaving radiances over extended areas. Therefore, improved atmospheric correction algorithms must be developed for the remote sensing of Case 2 waters [1], [5].

In this paper, we have proceeded to make the atmospheric correction of the eight multispectral bands of WV2 satellite by the 6S atmospheric correction model, based on the radiative transfer theory [17], [18]. 6S is an advanced radiative transfer code designed to simulate the reflection of solar radiation by a coupled atmosphere-surface system for a wide range of atmospheric, spectral, and geometrical conditions. The implemented algorithm provides patterns, which properly describe atmospheric conditions in these specific study areas, for monitoring shallow-water environments. This model, which is used by NASA for the correction of MODIS images, predicts the reflectance ρ of objects at the top of atmosphere (TOA), using information about the surface reflectance and atmospheric conditions. The TOA reflectance $\rho_{\text{TOA},\lambda}$ can be estimated using the following expression:

$$\rho_{\text{TOA},\lambda} = \frac{L_\lambda \cdot d^2 \cdot \pi}{E_\lambda \cdot \cos \theta_i}. \tag{1}$$

---

[1]The National Aeronautics and Space Administration's (NASA) Earth Observatory best satellite image of Earth 2013 (Canary Islands off the northwest coast of Africa, captured by NASA's Terra satellite June 2013).

[2]Declared in its entire biosphere reserve by UNESCO, May 26, 2009.

The minimum data sets needed to run the 6S model are the meteorological visibility (aerosol optical thickness), type of sensor, sun zenith and azimuth angles, date and time of image acquisition, and latitude–longitude of scene center. The top-of-canopy $\rho_{\mathrm{TOC},\lambda}$ is obtained from the model output by

$$\rho_{\mathrm{TOC},\lambda} = \frac{y}{1 + (x_c * y)} \quad y = (x_a * L_\lambda) - x_b \quad (2)$$

where $\rho_{\mathrm{TOC},\lambda}$ is the atmospheric corrected reflectance; L_λ is the sensed radiance; x_a, x_b, and x_c are the coefficients obtained from the aerosol concentration, spectral band, and ground reflectance, respectively.

Finally, in order to check the proper functioning of the selected 6S atmospheric correction algorithm, we used ground-based spectral data collected by the spectroradiometer Vis/NIR ASD FieldSpec 3 nearly coincident (similar weather and lighting conditions) with WV2 satellite overflight. The spectroradiometer main characteristics are the spectral range of 350–2500 nm; the spectral resolution of 3 nm at 700 nm and 30 nm at 2100 nm; and the sample interval of 1.4 nm at 700 nm and 2 nm at 2100 nm.

Fig. 3(a) shows a WV2 image from Port of Granadilla Environmental Monitoring Program Database, where *in situ* radiometric test points were obtained. The results obtained by 6S atmospheric correction techniques (% reflectivity) on the WV2 image compared with ground-based reflectance measurements are presented in Fig. 3(b). As it can be observed, results show a great correlation between the reflectivity values obtained by *in situ* measurements and the corresponding values obtained by the eight multispectral satellite channels through the 6S atmospheric model.

Fig. 3. (a) Location of *in situ* test points on WV2 imagery (February 2012) in Granadilla area and (b) ground-based reflectance measurements (top) and corresponding WV2 multispectral 6S atmospheric correction reflectance (bottom).
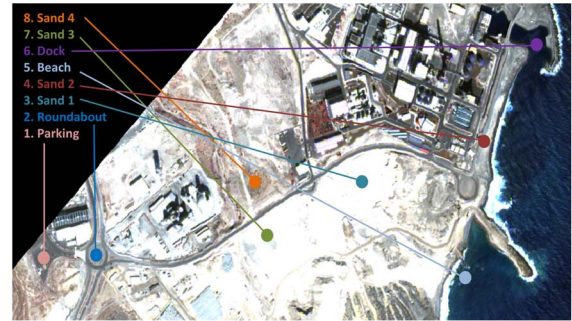
B. Sunglint Correction Algorithm

Specular reflection of solar radiation on nonflat water surfaces is a serious confounding factor for bathymetry retrieval in shallow-water environments. Therefore, the remote oceanographic features can be seriously impeded by the state of the water. Thus, we propose a method based on combined physical principles and image processing techniques for removal of sea surface effects from high-resolution imagery in coastal environments. Following the physical approach suggested in [7], one or more regions of the image are selected where a range of sunglint is evident, but where the underlying spectral brightness would be expected to be consistent, i.e., areas of deep water. For each visible band, all the selected pixels are included in a linear regression (b_i) of NIR (WV2 channels: 6, 7, and 8) brightness against the visible band brightness,
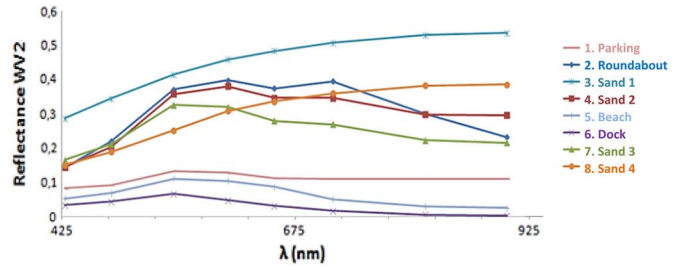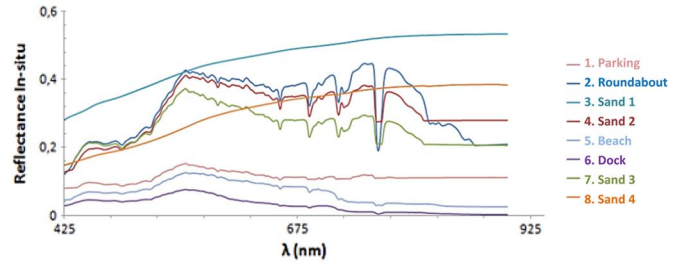
$$\rho_{\mathrm{TOC}}^{\mathrm{deg}}(\lambda) = \rho_{\mathrm{TOC}}(\lambda) - b_\lambda(\rho_{\mathrm{NIR}} - MIN\rho_{\mathrm{NIR}}) \quad (3)$$

$$R_{\mathrm{rs}}(\lambda) = \frac{\rho_{\mathrm{TOC}}^{\mathrm{deg}}(\lambda)}{\pi} \, sr^{-1} \quad (4)$$

$$r_{\mathrm{rs}}(\lambda) = \frac{R_{\mathrm{rs}}(\lambda)}{0.5\pi + 1.5 R_{\mathrm{rs}}(\lambda)} \quad (5)$$

where $\rho_{\mathrm{TOC}}^{\mathrm{deg}}(\lambda)$ is the deglinted surface reflectance; R_{rs} is the over-surface deglinted reflectivity; and r_{rs} is the subsurface reflectivity. After the physical approach, two image processing improvements have been developed.

1) A histogram-matching technique is applied to statistically equalize images, after deglinting, from the original water reflectivity for each channel due to that the previous deglinting process, in the presence of large waves, affects to the spectral content of the image, altering the reflectance intensity. The histogram matching allows statistical matching of images, after deglinting, with the theoretical reflectivity of water for each channel. The result is very suitable since the variation of the reflectivity is a normal function. That way, the foam of the waves or "whitecaps" can be removed and such pixels filled by interpolation.

2) Given that not all the WV2 sensor bands precisely capture the energy at the same time, using two multispectral channel groups in the acquisition, a further improvement in the glint removal algorithm has been performed, consisting in the use of the two channel groups separately using each NIR channel of the groups and the use of a
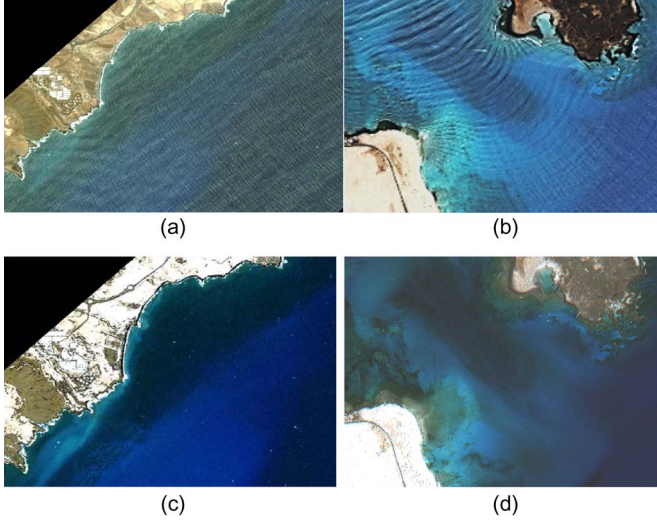
Fig. 4. (a) and (b) WV2 image of Granadilla and Corralejo area (August 2010/October 2010, wind speed of 5.5 and 4.2 m/s, respectively). (c) and (d) Image after the deglinting process.

sliding window, where template matching [2] techniques have been applied in order to eliminate the small spatial misalignments between bands.

The result of the full-deglinting algorithm is shown in Fig. 4. This example presents an atmospherically corrected WV2 multispectral imagery from the Granadilla and Corralejo areas, respectively, with pronounced glint over the sea surface, as shown in Fig. 4(a) and (b). After the glint was removed, subsurface features became pronounced and the bathymetry algorithm could be successfully applied [see Fig. 4(c) and (d)].

III. BATHYMETRY MAPPING OF SHALLOW-WATER ENVIRONMENTS

The problem of estimating water depths and water property monitoring requires frequent ship surveys. Specifically, the traditional bathymetry requires frequent oceanographic vessel surveys providing detailed information about the chosen sites, but it cannot show what happens to the broader coastal environment. Hence, there is an obvious need for measurements of water depth, particularly in shallow-water environments. To study the properties of the broad coastal environment instead of a few chosen sites, repetitive measurements by satellite sensors offer an attractive alternative. However, to adequately monitor complex coastal environments via multispectral scanner technology requires not only sophisticated sensors but also advanced data processing algorithms [9]–[11]. In our context, for bathymetry mapping, an efficient multichannel physics-based algorithm has been implemented, which is capable of solving through optimization the radiative transfer model of seawater. Using the radiative model to compute bathymetry has yielded good results and will allow to improve the outcome of the ratio algorithm as it considers the physical phenomena of water absorption and backscattering (K_d) and the relationship between the seafloor albedo, its depth, and the water intrinsic optical properties (IOPs). Thus, the radiative transfer equation

allows us to model the reflectivity and can be expressed by [19]–[21]

$$r_{\rm rs}^m \approx r_{\rm rs}^{\rm dp} \left(1 - e^{-\left[\frac{1}{\cos(\theta_s)} + \frac{D_u^c}{\cos(\theta_v)} \right] k_d z} \right)$$
$$+ \frac{\rho}{\pi} e^{-\left[\frac{1}{\cos(\theta_s)} + \frac{D_u^b}{\cos(\theta_v)} \right] k_d z} \qquad (6)$$

where $r_{\rm rs}^m$ is the modeled subsurface reflectivity; $r_{\rm rs}^{\rm dp}$ is the subsurface reflectivity of the deep water; ρ is the seafloor albedo; θ_s is the subsurface solar zenith angle; θ_v is the subsurface view angle; D_c^u and D_u^b are the optical path-elongation factors for scattered photons from the water column and the bottom, respectively; K_d is the diffuse attenuation coefficient; and Z is the depth.

The radiative transfer equation parameters depend greatly on the optical properties of the water expressed by [20], [22]

$$r_{\rm rs}^{\rm dp}(\lambda) \approx (0.084 + 0.17u(\lambda))u(\lambda) \qquad (7)$$

$$u(\lambda) = \frac{b_b(\lambda)}{a(\lambda) + b_b(\lambda)} \qquad (8)$$

$$k_d(\lambda) = a(\lambda)b_b(\lambda) \qquad (9)$$

$$D_u^c(\lambda) \approx \sqrt{1.03(1 + 2.4u(\lambda))} \qquad (10)$$

$$D_u^b(\lambda) \approx \sqrt{1.04(1 + 5.4u(\lambda))} \qquad (11)$$

$$b_b(\lambda) = b_{\rm bw}(\lambda) + \varepsilon(\lambda)b_{\rm bp}(\lambda) \qquad (12)$$

$$a(\lambda) = a_w(\lambda) + a_p(\lambda) + a + g(\lambda) \qquad (13)$$

$$\varepsilon(\lambda) \approx 1 + \left[0.1 + \frac{0.8b_{\rm bp}(\lambda)}{b_b(\lambda)} \right] \sin(\theta_s)\sin(\theta_v) \qquad (14)$$

where u is the backscattering diffuse attenuation ratio; a, a_w, a_p, a_g are the attenuation coefficients for water, phytoplankton, and gelbstoff; b_b, $b_{\rm bw}$, $b_{\rm bp}$ are the backscattering coefficients for water and particles; and ε is an empirical parameter to account the effect of changing angle on the effective scattering.

The attenuation and backscattering IOP parameters depend on the wavelength of each channel, a_w and b_w are tabulated values, while the other parameters can be modeled by wavelength functions as follows:

$$a_p(\lambda) = [a_0(\lambda) + a_1(\lambda) + a_1(\lambda)\ln(P)]P \qquad (15)$$

$$a_g(\lambda) = Ge^{-0.015(\lambda-440)} \qquad (16)$$

$$b_{\rm bp}(\lambda) = X\left(\frac{400}{\lambda} \right)^Y \qquad (17)$$

where a_0 and a_1 are the tabulated empirical coefficients for each channel; $P = a_p(440)$; $G = a_g(440)$; $X = b_{\rm bp}(400)$; Y is the spectral shape that depends on the particulate shape and size.

The water IOP $k_d(490)$ parameter for the WV2 was obtained and validated in [22], for the operational algorithm developed based on the relationship at the blue–green–yellow–red reflectance channels. Specifically, we have derived the
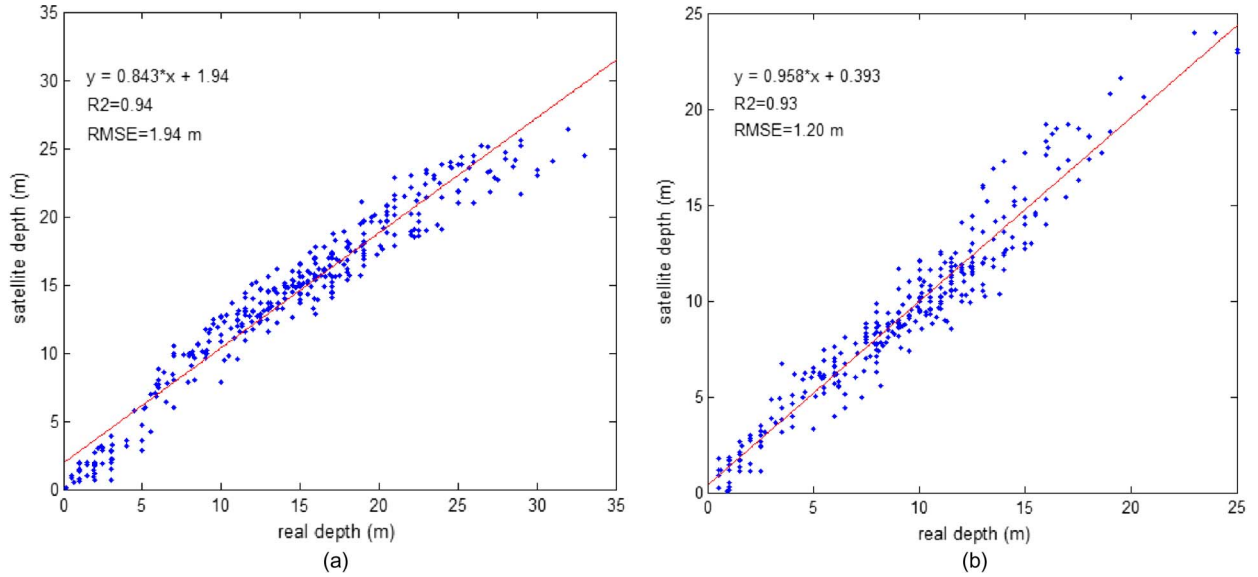
Fig. 5. Scatter plot showing bathymetry-algorithm-predicted depth versus acoustic depth from field data points for (a) Granadilla and (b) Corralejo area image data (best fit line in red).

high-resolution K_d product, using MODIS/MERIS data, *in situ* measurements, and the quasi-analytical algorithm (QAA) radiative transfer model for the WV2 channels [22]

$$\rho(\lambda) = B \times \rho_{\rm sd}(\lambda) \qquad (18)$$

where $\rho_{\rm sd}$ is the 550-nm-normalized sand-albedo shape; B is the bottom albedo at 550 nm. With these equations, there are six variables to be inverted. In this paper, the bathymetry estimation is based on the radiative modeling using a system of six equations

$$r_{\rm rs}^m(\lambda) = f[P, G, X, Y, B, Z] \qquad (19)$$

$$MIN_{\rm optimization} = \sum_{ch_1}^{ch_6} \{r_{\rm rs}^m(ch) - r_{\rm rs}(ch)\}^2. \qquad (20)$$

In the implementation of the gradient optimization algorithm, the Levenberg–Marquardt (LMA) method was used for solving the nonlinear equations [23]. The initialization of the Z parameter has been performed using the ratio algorithm result, for better and faster optimization convergence. The use of six bands (coastal blue, blue, green, yellow, red, and red edge) increases the spectral information, allowing the reflectance unmixing of the water IOPs and the depth–seafloor reflectance. This fact allows more precise bathymetry calculation at greater depths.

In Fig. 5, the accuracy of the proposed bathymetry retrieval algorithm output for each coastal area image was assessed with a scatter plot of the algorithm output versus acoustic field data obtained in [24] (including lineal fit, R^2, and RMSE). The derived satellite bathymetry RMSE is 1.20 and 1.94 m with R^2 between 0.93 and 0.94, for Granadilla and Corralejo areas, when compared with 350 and 318 acoustic measurements, over a range of $\sim$1 to $\sim$30 m, respectively. The results of seafloor albedo and bathymetry for the selected Canary Islands littoral zones [see Fig. 6(a)] are presented in Fig. 6(b) and (c), respectively.

IV. BENTHIC HABITAT MAPPING

Monitoring benthic habitats provides an important insight into the health of marine ecosystems, in general, and in particular, seagrass is a keystone of coastal marine life, providing critical habitats and nutrients to fisheries. In Canary Islands, as well as other parts of the world, coastal seafloor benthic habitats (and seagrass density) have traditionally been mapped from aerial photography, using photointerpretation techniques, or using *in situ* measurements (bionomic maps obtained with oceanographic ships) [24]–[26].

In recent years, there has been an increase in the availability and affordability of high spatial resolution satellite imagery (i.e., WV2 data), providing a more cost-effective solution for attaining source data to map benthic habitats [11], [26].

There are various types of benthic-habitat-mapping techniques based on satellite imagery and remote sensing data, which have been proved to be effective [27], [28]; however, results of high-resolution imagery-based benthos classification are affected by water column effects. In the water column, the dynamic inherent optical properties of light absorption and scattering change the spectral response of seafloor features over space and time, complicating the benthic mapping process [10]–[12]. Absorption and scattering of light in the water column are caused not only by suspended materials (i.e., during the works of the port of Granadilla); the water itself exponentially decays light intensity with increased water depth (light attenuation). These water column properties create spectral inconsistencies, which must be accounted for during image classification. These spectral variations can cause misclassifications in spectral classification routines [29].

Implementation of water-column light-attenuation-correction routines can improve the results of benthic habitat classification algorithms. Light attenuation corrections can create depth-independent bottom reflectance images, where similar features have similar reflectance values [8], [11], [20], [21]. With adequate bathymetric information, correction coefficients can be
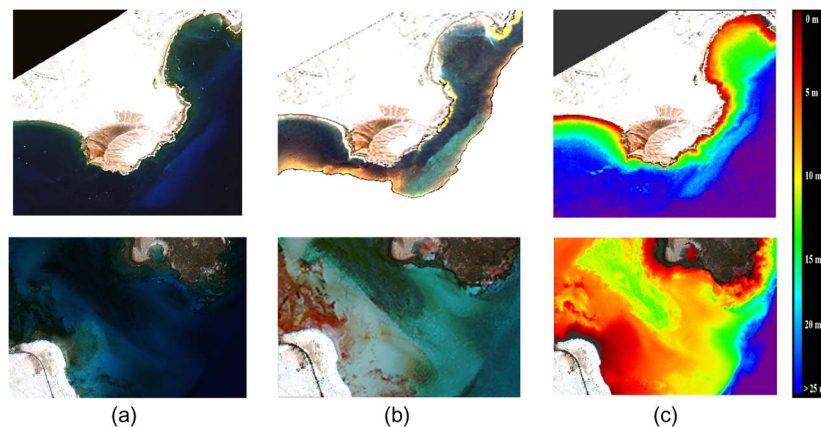
Fig. 6. Selected areas on the WV2 images of Tenerife and Fuerteventura (Canary Islands) coastal area. (a) Atmospheric and sunglint corrected imagery, (b) seafloor albedo (coastal blue-green-blue bands), and (c) maps of estimated depth (bathymetry).

calculated for each band by comparing pixels of known bottom types at different depths as a depth variant light attenuation correction [30]. The use of a water column correction will improve the accuracy of benthic mapping by minimizing the influence of the water column and allowing for the dominant spectral signature to be attributed to the benthos.

The accuracy of image classification depends on the spectral and spatial resolution of the data. Therefore, the proposed benthic-habitat-mapping technique performs an extraction and normalization of benthic indexes that matches the seafloor reflectivity and estimated bathymetry with their related coastal seafloor benthic habitats. Afterward, a supervised classification methodology, combined with the additional information provided by the normalized benthic indexes, has been implemented for benthic habitat mapping. Therefore, there are two different steps that must be addressed: extraction of normalized benthic indexes and robust classification of shallow environments from the high-resolution imagery.

A. Seafloor Normalized Indexes

From the reflectivity map of the seafloor, generated by the multiresolution radiative transfer model algorithm detailed in Section III, we obtained normalized indexes to detect and interpret the different types of benthos and seabed. Using indexes is a well-known transformation, in particular for the estimation of land vegetation cover [30]–[32]. In our case, the use of normalized benthic indexes, in addition to the seabed reflectivity, will improve the results of the classification procedure, since this preprocessing increases the class separability and, in consequence, the classifier performance. Furthermore, the use of bathymetric information, when obtaining the seafloor indexes, provides another important source of information on the classification since benthic classes are stratified with depth [32].

From the reflectivity and bathymetry images, as shown in Fig. 6(b) and (c) for the study area, normalized seafloor indexes have been determined, using the expressions given in Table I, for the three classes of interest: seagrass, sand, and maerl [33], [34]. Table I includes, as well, an example of the seafloor indexes obtained for the area of Granadilla.

In Table I, $r1$, $r2$, and $r3$ are the seafloor reflectivity for coastal blue, blue, and green WV2 multispectral bands, respectively, and z is the bathymetry (in meters).
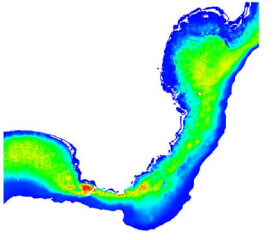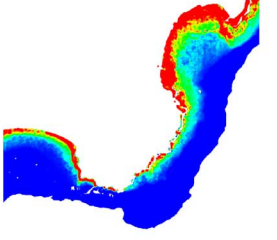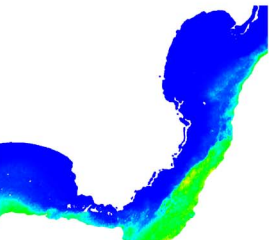
B. Classification of Benthic Habitats

High-spatial-resolution imagery leads to new image processing challenges and offers new opportunities for potentially more accurate detection and classification as compared to previously available satellite imagery. Many methods have been developed to classify digital images using the spectral, spatial, or temporal properties of the objects present in the images [2], [13].

In the past decades, a great effort has been devoted to exploit machine learning methods for classification. In particular, neural networks were introduced for solving different classification tasks using different models [multilayer perceptron networks, radial basis functions (RBFs), etc.]. The previous learning theory is at the basis of the SVM approach. The SVM [13], [35] has proven to be very effective in solving complex remote sensing classification problems, mainly due to the fact that this technique does not require an estimation of the statistical distribution of classes to carry out the classification task and exploits a model based on the concept of margin maximization. This is particularly useful because data acquired from remotely sensed imagery usually have unknown distributions. Thus, this allows SVMs to outperform techniques based on maximum-likelihood classification because, in general, it is not a correct assumption of the actual pixel distribution in each class [36]. An additional aspect about SVMs is their ability to limited amount or quality of training samples [35]. This property has been exploited and has proved to be very useful in many of the applications such as seafloor mapping, mainly, because acquisition of ground truth is generally an expensive process.

The mapping of benthic habitats is a very challenging problem because only very few spectral information is available for the classification. In fact, depending on the depth to analyze, only three to four WV2 bands could be useful. In this context, the SVM combined by the additional information provided by the benthic indexes can be an effective methodology for the robust classification of shallow environments.

TABLE I
SEAFLOOR NORMALIZED INDEXES FOR SEAGRASS, SAND, AND MAERL

Seafloor category	Determination of seafloor normalized indexes [0-1]	Indexes for study area
Seagrass	$NSI = \left(\left[\frac{r3-r1}{r3+r1}\right]_0^{0.3} * 3.33\right)$ $* \left(cos^2\left(\frac{\frac{\pi}{2} * ([abs(0.12-r1)]_0^{0.1} + [abs(0.20-r3)]_0^{0.1})}{2*0.1}\right)\right)$ $* \left(cos\left(\frac{\frac{\pi}{2} * [(10+z)]_{-10}^{+10}}{20}\right)\right)$	
Sand	$NAI = \left(\frac{[r2-0.15]_0^{0.15} + [r3-0.2]_0^{0.15}}{0.3}\right)$ $* \left(cos^2\left(\frac{\frac{\pi}{2} * [(5+z)]_{-5}^{+0}}{7}\right)\right)$	
Maerl	$NMI = \left(\left[1 - \frac{r3-r1}{r3+r1}\right]_0^1\right)$ $* \left(\frac{[r2-0.2]_0^{0.25} + [r3-0.3]_0^{0.25}}{0.5}\right)$ $* \left(cos\left(\frac{\frac{\pi}{2} * [(16+z)]_0^6}{7}\right)\right)$	

In our work, the SVM kernel and parameter selection was done according to the conclusions in [37]–[39], which state that, for land cover classification, the RBF kernel is a suitable choice, which provided better accuracy than polynomial and sigmoid kernels. As we deal with a supervised technique, and for the accuracy evaluation stage, *in situ* data were required. Data used for these training and validation purposes were provided by the Observatorio Ambiental Granadilla from transects performed in September 2012, by the visual information collected in selected test stations (January 2013), and by the Centro de Investigaciones Medioambientales del Atlántico (CIMA) bionomical map [25] made in the area in 2008, as shown in Fig. 7.

As indicated, for the mapping of benthic features, a supervised SVM classification has been carried out using the available multispectral data, after atmospheric and sunglint corrections, plus the estimated benthic indexes. The training classes and regions of interest were clearly defined, and a detailed separability assessment was conducted using the Jeffries–Matusita metric [40]. Due to the limited number of available bands, separability values were, in general, low for the majority of class pairs, indicating the complexity to perform a precise classification.
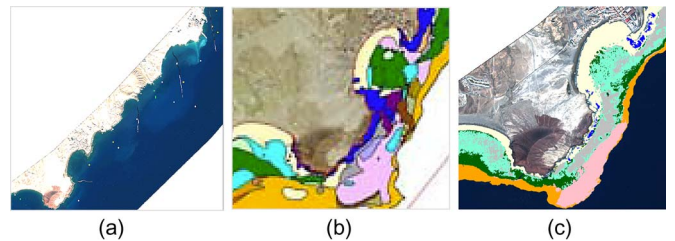

Fig. 7. (a) Location of the test stations and transects. (b) CIMA 2008 map of benthic habitats for the area of Granadilla (seagrass in green and light blue, sand in yellow and orange, maerl in pink, and algae in blue). (c) Classification map obtained by the combination of benthic indexes and SVM supervised classification (seagrass in green, sand in yellow and orange, maerl in pink, and algae in blue).

Fig. 7(c) shows the classification results for a selected area of the Granadilla image (sparse and dense seagrass are included in light and dark green, respectively, and shallow and deeper sand are presented in yellow and orange). Based on the results, a high correlation can be appreciated between the benthic vegetation mapping derived from satellite and the corresponding CIMA bionomical map provided. Class colors have been selected to approximately match those contained in the CIMA map. Using
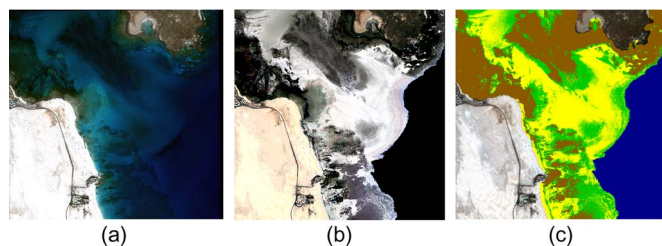
Fig. 8. Corralejo area. (a) True color composite after atmospheric correction and deglinting. (b) Seabed reflectivity after water column correction. (c) Classification map (seagrass in green, sand in yellow, rocks in brown, and deep waters in blue).

the data collected during transects and by test stations, a quantitative estimation of the classification accuracy was computed. Results are consistent with available bionomic profiles, and the overall accuracy achieved was 73% with a kappa coefficient of 0.716.

Fig. 8 displays the results for the Corralejo area. We can appreciate that, after the water column correction [see Fig. 8(b)], the seabed classes are enhanced and can be better identified. Fig. 8(c) shows the resulting thematic map (seagrass in green; sandy and rocky areas in yellow and brown, respectively; and deep water in blue) using the SVM classifier with the RBF kernel. We can notice that regions having a water depth over 25 m have been masked because a reliable estimation of the seafloor is difficult to achieve.

It is important to emphasize that the mapping of shallow coastal areas using high-resolution imagery is a very complex and challenging task since only those WV2 channels with higher penetration channels can be used. Thus, the need to cover depths near 20 m allows only the use of bands in the blue–green range. This fact clearly limits the classification possibilities due to the low variability of the different types of seafloor in these channels, which results in a low separability of classes to be discriminated. In addition, the very low level of the signal sensed by the sensor, in comparison with the many contributions of noise present in the images (atmosphere, solar reflection, foam, turbidity, etc.), imposes a large number of restrictions on the successful use of benthic mapping algorithms. Regardless of previous inconveniences, the results achieved by our classification methodology have been satisfactory and agree fairly well with the available field data.

V. CONCLUSION

Given the importance of the coastal ecosystems for life quality and the global climate, efficient and adequate information about the biogeochemical contents, water clarity, bathymetry, and distribution of benthic habitats of coastal ecosystems is important for government agencies and the public. Satellite-based imaging systems with spectral bands within the visible spectrum reliably provide information at spatial scales needed to implement spatially based conservation actions for coastal locations, such as the Granadilla Environmental Monitoring Program and Corralejo Marine Protected Area, and they enable observations of the coastal parameters at greater spatial and finer temporal scales than those allowed through field observa-

tion alone. This work has demonstrated the application of very high-resolution multispectral imagery to estimate bathymetry and distribution of benthic habitats in the shallow-water environments.

For the high spatial resolution WV2 data preprocessing strategy, this study affirms that atmospheric correction and deglinting methods should be applied to WV2 imagery prior to the development of bathymetric and benthic maps, in order to increase the accuracy of the final products. Preprocessing methods alter the estimated radiance and reflectance values to account for known sources of error in the data, resulting in values that more closely estimate the true radiance and reflectance. The most common method for evaluating atmospheric correction is to compare the retrieved reflectance from satellite images with ground-based measurements for a variety of targets. We compared the 6S model with coincident ground-based reflectance measurements in the area under study areas, obtaining a very good correlation between the reflectivity values obtained by *in situ* measurements and the corresponding values acquired by atmospheric processing of the eight multispectral satellite channels. Thus, it is not surprising that applying both preprocessing procedures prior to fitting the depth derivation model improved the retrieved water depths.

For bathymetry retrieval, an efficient multichannel physics-based model has been implemented. The sophisticated model developed and evaluated in this study expands the ratio algorithm model, allowing for the increased amount of information provided in WV2 imagery to be included in the retrieval of water depth. The enhanced capacity provided by the WV2 imagery, coupled with the new model presented herein, has a greater precision in water-depth retrievals. While the developed model reproduced depths up to approximately 25 m, a threshold (mask) around 25–30 m indicated failure of the prediction. These results suggest excellent retrieval of bathymetry from high-resolution multispectral remote sensing imagery.

Efficient and effective mapping techniques are crucial to managing coastal resources at a regional scale using very high-resolution imagery. However, the mapping of benthic habitats is a complex problem because only limited and noisy spectral information is available. In this context, the use of seafloor normalized indexes, which take into account bathymetric information, provides improved performance, with respect to classical classification methods directly applied to the seafloor albedo or spectral bands. Pixel-based supervised classification has been applied with the combination of the benthic indexes using the nonparametric SVM approach with the Gaussian RBF kernel. After a qualitative evaluation and once compared with ground truth data, an overall accuracy over 70% has been achieved. Thus, we can conclude that the presented methodology has demonstrated a good performance for the robust classification of shallow environments, taking into account the existing difficulties and limited spectral data available.

In summary, satellite remote sensing has provided a systematic and a synoptic framework for improving the scientific knowledge about the littoral zones and, in particular, has demonstrated the application of high-resolution multispectral remote imagery to remote bathymetry and benthic mapping of shallow-water environments. High-resolution regionally
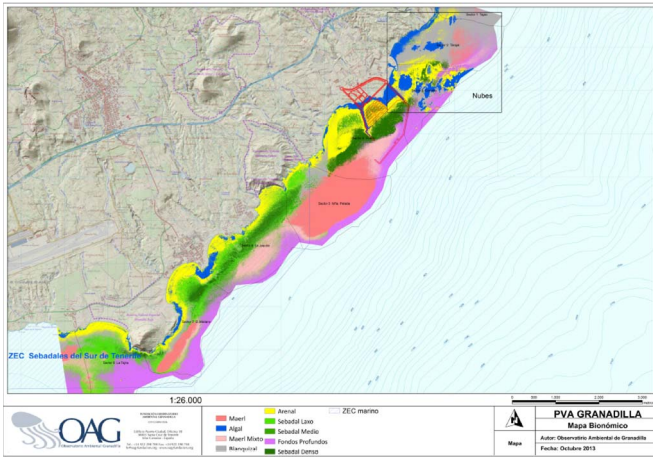
Fig. 9. Satellite high-resolution map of benthic habitats obtained by the implemented WV2 multispectral remote sensing methodology in the framework of the Port of Granadilla Environmental Monitoring Program (October 2013).

optimized maps of coastal areas have been validated with *in situ* data and available bionomic profiles.

It is important to emphasize that our methodology is currently being used operationally in the frame of the Multitemporal European Monitoring Program for Port of Granadilla (Tenerife Island). To that respect, Fig. 9 includes one example of the official benthic map generated in October 2013.

Continued research on the use of advanced image processing techniques [for example, object-based image analysis (OBIA) classification] and their transferability to other locations and satellite products is needed to strengthen the integration of image processing techniques in operational benthic mapping projects. These progressive improvements have been developed, and some are underway as part of projects such as ARTEMISAT and TELECAN, which are funded by the Spanish Government and the European Commission, respectively.

The periodic bathymetry and benthic maps for monitoring Granadilla environment are produced from remote sensing data, which provide encouragement to management agencies for investing in the use of satellite as a monitoring, mapping, and management tool.

REFERENCES

[1] Y. Wang, *Remote Sensing of Coastal Environments*, Taylor and Francis Series in Remote Sensing Applications. Boca Raton, FL, USA: CRC Press, 2010.

[2] J. A. Richards, *Remote Sensing Digital Image Analysis*. Berlin, Germany: Springer-Verlag, 2013.

[3] R. L. Miller, C. Del Castillo, and B. McKee, *Remote Sensing of Coastal Aquatic Environments*. New York, NY, USA: Springer-Verlag, 2005.

[4] E. P. Green, P. J. Mumby, A. J. Edwards, and C. D. Clark, *Remote Sensing Handbook for Tropical Coastal Management*. Paris, France: UNESCO, 2000.

[5] S. Abdolrassoul, B. Mahiny, and J. Turner, "A comparison of four common atmospheric correction methods," *Photogramm. Eng. Remote Sens.*, vol. 73, no. 4, pp. 361–368, Apr. 2007.

[6] S. M. Adler-Golden, P. A. Acharya, A. Berk, M. Matthew, and D. Gorodetzky, "Remote bathymetry of the littoral zone from AVIRIS, LASH and QuickBird imagery," *IEEE Trans. Geosci. Remote Sens.*, vol. 43, no. 2, pp. 337–347, Feb. 2005.

[7] S. Kay, J. Hedley, and S. Lavender, "Sun glint correction of high and low spatial resolution images of aquatic scenes: A review of methods for visible and near-infrared wavelengths," *Remote Sens.*, vol. 1, no. 4, pp. 697–730, 2009.

[8] D. R. Lyzenga, N. P. Malinas, and F. J. Tanis, "Multispectral bathymetry using a simple physically based algorithm," *IEEE Trans. Geosci. Remote Sens.*, vol. 44, no. 8, pp. 2251–2259, Aug. 2006.

[9] A. Collin and J. L. Hench, "Towards deeper measurements of tropical reefscape structure using the WorldView-2 spaceborne sensor," *Remote Sens.*, vol. 4, no. 5, pp. 1425–1447, 2012.

[10] L. Zhongping *et al.*, "Water and bottom properties of a coastal environment derived from Hyperion data measured from the EO-1 spacecraft platform," *J. Appl. Remote Sens.*, vol. 1, no. 1, Jan. 2007, Art. ID. 011502.

[11] M. Lyons, S. Phinn, and C. Roelfsema, "Integrating Quickbird multispectral satellite and field data: Mapping bathymetry, seagrass cover, seagrass species and change in Moreton Bay, Australia in 2004 and 2007," *Remote Sens.*, vol. 3, no. 1, pp. 42–64, 2011.

[12] F. Eugenio, J. Martin, J. Marcello, and J. A. Bermejo, "Worldview-2 high resolution remote sensing image processing for the monitoring of coastal areas," in *Proc. 21st Eur. Signal Process. Conf.*, Marrakech, Morocco, Sep. 9–13, 2013, pp. 1–5.

[13] B. Tso and P. M. Mather, *Classification Methods for Remotely Sensed Data*. New York, NY, USA: Taylor & Francis, 2009.

[14] T. Updike and C. Comp, A Radiometric Use of WorldView-2 Imagery, Technical Note, 2010.

[15] P. S. Chavez, Jr., "Image-based atmospheric corrections. revisited and improved," *Photogramm. Eng. Remote Sens.*, vol. 62, no. 9, pp. 10257–1036, Sep. 1996.

[16] G. Doxani, M. Papadopoulou, P. Lafazani, M. Tsakiri-Strati, and E. Mavridou, "Sun glint correction of very high spatial resolution images," in *Thales, in Honor of Prof. Emeritus Michael E. Contadakis*, 329–340, 2013. [Online]. Available: http://www.topo.auth.gr/greek/ORG_DOMI/EMERITUS/TOMOS_CONTADAKIS/Thales_pdf/3.01_Doxani.pdf

[17] E. F. Vermote, D. Tanré, J. L. Deuzé, M. Herman, and J. Morcrette, "Second simulation of the satellite signal in the solar spectrum, 6S: An overview," *IEEE Trans. Geosci. Remote Sens.*, vol. 35, no. 3, pp. 675–686, May 1997.

[18] Y. Svetlana *et al.*, "Validation of vector version of 6s radiative transfer code for atmospheric correction of satellite data. Part I. Parth radiance," *Appl. Opt.*, vol. 45, no. 26, pp. 6762–6774, Sep. 2006.

[19] S. Maritorena, A. Morel, and B. Gentilly, "Diffuse reflectance of oceanic shallow waters: Influence of water depth and bottom albedo," *Limnol. Oceanography*, vol. 39, no. 7, pp. 1689–1703, 1994.

[20] L. Zhonping, "Hyperspectral remote sensing for shadow waters: 2. Deriving bottom depths and water properties by optimization," *Appl. Opt.*, vol. 38, no. 18, pp. 3831–3843, Jun. 1999.

[21] V. E. Brando *et al.*, "A physics based retrieval and quality assessment of bathymetry from suboptimal hyperspectral data," *Remote Sens. Environ.*, vol. 113, no. 4, pp. 755–770, Apr. 2009.

[22] F. Eugenio, J. Martin, J. Marcello, and E. Fraile-Nuez, "Environmental monitoring of El Hierro Island submarine volcano, by combining low and high resolution satellite imagery," *Int. J. Appl. Earth Observ. Geoinform.*, vol. 29, pp. 53–66, Jun. 2014.

[23] H. P. Gavin, "The Levenberg-Marquardt method for nonlinear least squares curve-fitting problems," Dept. Civil Environ. Eng., Duke Univ., Durham, NC, USA, Oct. 2013.

[24] Integrated Marine Data Repository for Macaronesia—REDMIC, Fundación Observatorio Ambiental de Granadilla (OAG). [Online]. Available: http://www.redmic.es/

[25] M. Rodríguez *et al.*, "Estudio Bionómico del Lugar de Interés Comunitario (LIC) Sebadales del Sur de Tenerife," C.I.M.A—Informe Técnico, 2008.

[26] R. Baumstarka, B. Dixon, P. Carlson, D. Palandro, and K. Kolasa, "Alternative spatially enhanced integrative techniques for mapping seagrass in Florida's marine ecosystem," *Int. J. Remote Sens.*, vol. 34, no. 4, pp. 1248–1264, 2013.

[27] E. Peneva, J. A. Griffith, and G. A. Carter, "Seagrass mapping in the northern Gulf of Mexico using airborne hyperspectral imagery: A comparison of classification methods," *J. Coastal Res.*, vol. 24, no. 4, pp. 850–856, Jul. 2008.

[28] A. Knudby and L. Nordlund, "Remote sensing of seagrasses in a patchy multi-species environment," *Int. J. Remote Sens.*, vol. 32, no. 8, pp. 2227–2244, 2011.

[29] S. R. Phinn, C. M. Roelfsema, and P. J. Mumby, "Multi-scale, object-based image analysis for mapping geomorphic and ecological zones on coral reefs," *Int. J. Remote Sens.*, 33, no. 12, pp. 3768–3797, 2012.

[30] J. Goodman and S. L. Ustin, "Classification of benthic composition in a coral reef environment using spectral unmixing," *J. Appl. Remote Sens.*, vol. 1, no. 1, 2007, Art. ID. 011501.

[31] S. J. Purkis, "A 'Reef-Up' approach to classifying coral habitats from IKONOS imagery," *IEEE Trans. Geosci. Remote Sens.*, vol. 43, no. 6, pp. 1375–1390, Jun. 2005.

[32] R. Darvishzadeh, A. Skidmore, M. Schlerf, and C. Atzberger, "Inversion of a radiative transfer model for estimating vegetation LAI and chlorophyll in a heterogeneous grassland," *Remote Sens. Environ.*, vol. 112, no. 5, pp. 2592–2604, May 2008.

[33] J. A. Goodman, S. J. Purkis, and S. R. Phinn, *Coral Reef Remote Sensing: A Guide for Mapping, Monitoring and Management*. New York, NY, USA: Springer-Verlag, 2013.

[34] Estudio Ecocartográfico del Litoral de las Islas de Fuerteventura y Lobos. Ministerio de Medio Ambiente, Secretaría General del Territorio y la Biodiversidad, Dirección General de Costas. Información General, Jun. 2006.

[35] G. Mountrakis, J. Im, and C. Ogole, "Support vector machines in remote sensing: A review," *ISPRS J. Photogramm. Remote Sens.*, vol. 66, no. 3, pp. 247–259, May 2011.

[36] L. Su and Y. Huang, "Support vector machine classification: Comparison of linkage techniques using a clustering-based method for training data selection," *GISci. Remote Sens.*, vol. 46, no. 4, pp. 411–423, 2009.

[37] T. Kavzoglu and I. Colkesen, "A kernel functions analysis for support vector machines for land cover classification," *Int. J. Appl. Earth Observ. Geoinf.*, vol. 11, no. 5, pp. 352–359, 2009.

[38] J. Marcello, F. Calderero, F. Eugenio, and F. Marqués, "Analysis of urban and vegetation growing in NW Senegal during the last 25 years using medium resolution imagery," in *Proc. IEEE Int. IGARSS*, Quebec, ON, Canada, Jul. 12–19, 2014, pp. 2197–2200.

[39] P. del Aguila, F. Calderero, F. Marqués, J. Marcello, and F. Eugenio, "Fast generation of LULC maps for temporal studies in NW Africa," in *Proc. IEEE IGARSS*, Quebec, ON, Canada, Jul. 12–19, 2014, pp. 4280–4283.

[40] M. J. Canty, *Image Analysis, Classification and Change Detection in Remote Sensing*. Boca Raton, FL, USA: Taylor & Francis, 2009.

Francisco Eugenio (M'00–SM'06) received the B.S., M.S., and Ph.D. degrees from the Universidad de Las Palmas de Gran Canaria (ULPGC), Las Palmas de Gran Canaria, Spain, in 1986, 1993, and 2000, respectively, all in electrical engineering.

In June 1996, he joined the Department of Signal and Communications, ULPGC. From 1998 to December 2000, he was with the Technical University of Catalonia (UPC), Barcelona, Spain, working in image processing. Since 2003, he has been an Associate Professor with ULPGC, where he served as the Dean of the Telecommunication School in 2004–2010 and is currently lecturing on the area of remote sensing and radar. His current research interests include remote sensing image processing focuses on new methodologies and algorithms for multispectral high-resolution remote sensing processing for the monitoring of shallow-water environments and fusion of multisensor/multiresolution satellite image data. In these areas, he is the author or coauthor of many publications that have appeared as journal papers and proceeding articles.

Javier Marcello (M'99–SM'12) received the M.S. degree in electrical engineering from the Technical University of Catalonia (UPC), Barcelona, Spain, in 1993 and the Ph.D. degree from the Universidad de Las Palmas de Gran Canaria (ULPGC), Las Palmas de Gran Canaria, Spain, in 2006.

From 1992 to 2000, he was the Head Engineer at the Spanish Aerospace Defense Administration (Instituto Nacional de Técnica Aeroespacial), serving at the Canary Space Center, for different programs (Cospas-Sarsat, TT&C, MINISAT, Helios, and CREPAD). In January 1994, he joined the Department of Signal and Communications, ULPGC, where he has been an Associate Professor in the Telecommunication School, lecturing on the areas of satellite and radio communications, since 1999. His research is conducted at the Institute of Oceanography and Global Change (ULPGC) and includes multisensor/multitemporal remote sensing image processing, particularly image segmentation, classification, fusion, and oceanographic and land product generation.

Javier Martin received the M.S. degree in electrical engineering from the University of Las Palmas of Gran Canaria, Las Palmas, Spain, in 2011 and currently working toward the doctorate degree in the Instituto de Oceanografía y Cambio Global (IOCAG).

He is currently with the Spanish Aerospace Defense Administration (Instituto Nacional de Tecnica Aeroespacial), Madrid, Spain. His research areas of interest include remote sensing image processing techniques (preprocessing, classification, segmentation, feature extraction, and motion estimation); coastal monitoring by remote sensing images with very high resolution (shallow-water-area analysis: bathymetry and benthic classification); water quality analysis using remote sensing images of medium resolution (open ocean water) and high resolution (shallow-water area) and high-resolution coregistration photogrammetry, and optical and synthetic aperture radar sensors modeling of very high resolution satellites.